Proceedings of the International Association for Shell and Spatial Structures (IASS) Symposium 2009, Valencia
Evolution and Trends in Design, Analysis and Construction of Shell and Spatial Structures
28 September – 2 October 2009, Universidad Politecnica de Valencia, Spain
Alberto DOMINGO and Carlos LAZARO (eds.)

Dynamic responses of cylindrical lattice shell roofs under horizontal earthquake motions with arbitrary direction by shaking table tests

Tomohiko KUMAGAI*, Toru TAKEUCHI[a], Izumi SUZUKI[b], Toshiyuki OGAWA[a]

* Dept. of Architecture and Building Engineering, Tokyo Institute of Technology
O-okayama 2-12-1-M1-34, Meguro-ku, Tokyo 152-8550, JAPAN
kuma@arch.titech.ac.jp
[a] Tokyo Institute of Technology, Tokyo, Japan
[b] Technology Development Division, Fujita Corporation, Kanagawa, Japan

Abstract

This paper is intended as an investigation of the seismic response behavior of cylindrical lattice shell structures by shaking table tests. The seismic vibration tests are carried out using small scale models with shell span of 60 cm of cylindrical lattice shell roofs with substructure under horizontal motions in arbitrary direction.

From the experimental results, the effects of difference of earthquake input direction and relationship between mechanical properties of roofs and substructures on response behavior of shell roofs are made clear. In addition, it is confirmed that the seismic response evaluation methods proposed in previous papers (Takeuchi *et al*. [1] ~ Takeuchi *et al*. [3]) apply to the responses subjected to earthquake motions with arbitrary direction.

Keywords: cylindrical lattice shell roof, substructure, natural period ratio, shaking table test, small scale model, horizontal earthquake motion, input in arbitrary direction, response acceleration amplification factor, seismic response evaluation method

1. Introduction

Seismic response of cylindrical lattice shell roofs with supporting substructures is known to be amplified in vertical direction even under horizontal input, and their amplitude changes along the direction of earthquake motion (Takeuchi *et al*. [1]). However, the seismic response behavior under the inputs in arbitrary direction has not been sufficiently investigated. In this paper, seismic vibration tests are carried out using small scale models with supporting substructure in order to make clear the effects of difference of input direction and relationship between mechanical properties of roofs and substructures on response behavior of shell roofs. In addition, it is confirmed that the seismic response evaluation methods pro-

posed in previous papers (Takeuchi *et al*. [1] ~ Takeuchi *et al*. [3]) apply to the responses subjected to earthquake motions with arbitrary direction.

2. Outlines of vibration tests

2.1. Specimens and experimental devices

The experimental models shown in Photo.1 and Fig.1 are the cylindrical lattice shell roofs with substructures. The names of models are shown at the right of Photo 1. The shape of shell roofs is shown in Fig.2. The models are the following 3 types. Fs model is the model of shell roof with substructure, Rs model is the model of shell roof without substructure and Es model is the equivalent single-mass model with mass of shell roof and substructure. The shell roof is made of cold rolled steel plates (SPCC) 0.8mm thick. The arch span L_x is 60

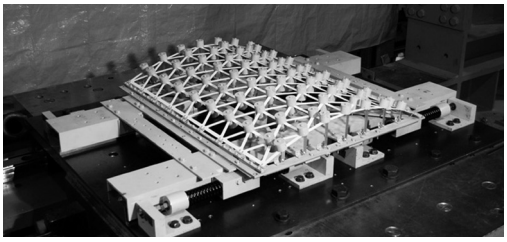

Photo 1: Experimental device of cylindrical lattice shell structure

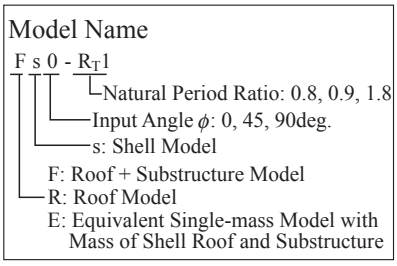

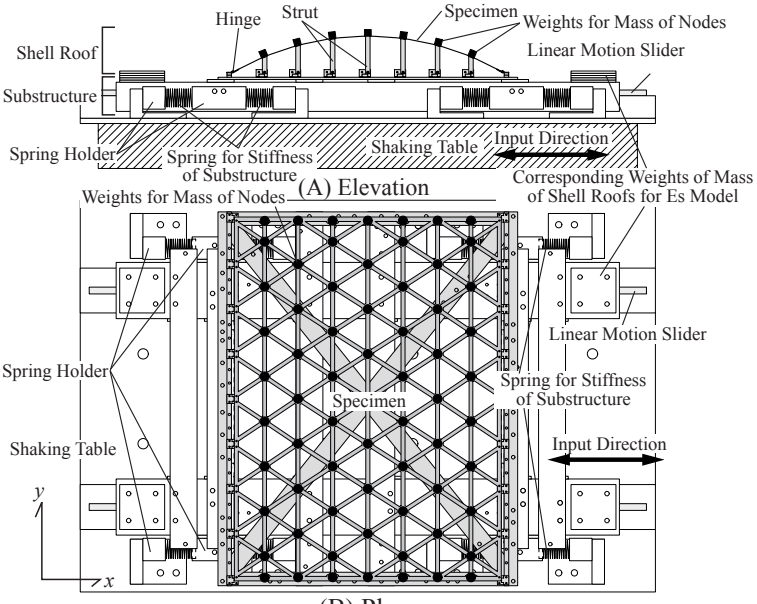

Figure 1: Experimental device (input angle ϕ=0deg.)

cm, the half subtended angle of shell is 30 degrees. The shell roofs are fixed with hinges, the boundary of roof is a pin support. The line connecting node A and node A' through node O is called "center line" and the line connecting node B and node B' is called "ridge". The substructures consist of a linear motion slider, compression springs and weights. The natural periods of substructures are adjusted by varying the spring constants. The ratios R_T of the natural period of Es model to that of antisymmetrical 1 wave mode(O1) of Rs0 model are adjusted to 0.8, 0.9 and 1.8. The brazen weights is attached to the nodes of shell for the purpose of lengthening the period of shell roof and the stresses occurring uniformly under the dead load as shown in Fig.3.

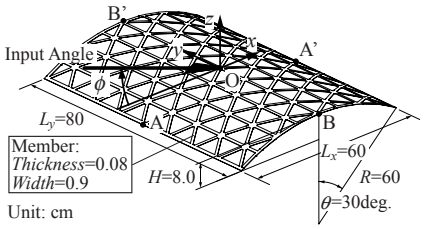

Figure 2: Shape of shell roof

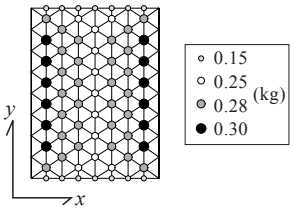

Figure 3: Distribution of brazen weights (shell roof)

2.2. Loading and measurement programs

The shell roofs are subjected to the horizontal earthquake motions with arbitrary direction. The input directions of earthquake motions are 0 deg. (gable (arch) direction), 90 deg. (longitudinal direction) and 45 deg. (oblique direction). The earthquake input direction is changed by rotating the only shell roof on substructure. The input earthquake motions are BCJ-L1 which is an artificial earthquake motion of the Building Center of Japan, El Centro NS (1940), Taft EW (1952), Hachinohe NS (1968) and JMA Kobe NS (1995). The time axes of earthquake motions are shortened in half. The maximum velocities of input earthquake motions are standardized to be 15 cm/sec. The shell roofs and substructures are in elastic range under these earthquake motions. The responses of structures are measured with the accelerometers, the motion capture systems (MC), the strain gauges and the laser displacement sensor. The positions for measurements are shown in Fig.4. The accelerations of shell structures are obtained by differentiating the measured displacements by MC twice with respect to time *t*. The accuracies of these accelerations are verified by comparison of the response values by the motion capture systems with those by the accelerometers.

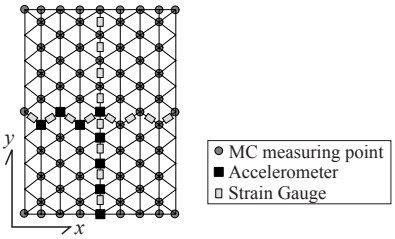

Figure 4: Positions of measuring points (shell roof)

3. Vibrational characteristics of cylindrical lattice shells

Fig.5 shows the natural vibrational characteristics for Rs model. The natural periods of Rs0 and Rs45 models are about 0.07 sec, those of Rs90 model are about 0.05 sec. The plural number of modes is measured in close range. The 2nd modes of Rs0 and Rs45 models are antisymmetrical 1 wave mode (O1, O1'). The 3rd mode of Rs0 model are antisymmetrical 2 wave mode (O2). In the case of Rs45 model, the asymmetrical mode with deformation at the center node O shown in Fig.6 is dominant mode.

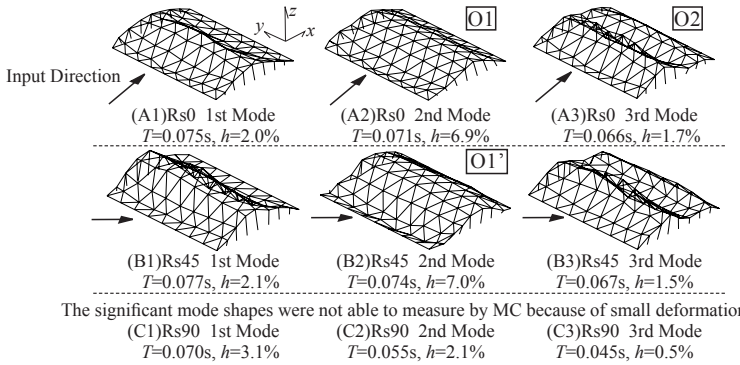

Figure 5: Natural vibrational characteristics (Rs model)

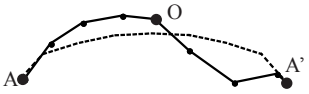

Figure 6: Mode shape of 2nd mode for Rs45 (AOA')

Next, the natural vibrational characteristics of Es (equivalent single-mass) model are examined. In the case of Es model, the amplitude dependence occurs in the relationships between the damping factors and the responses as shown in Fig.7. This behavior is described by

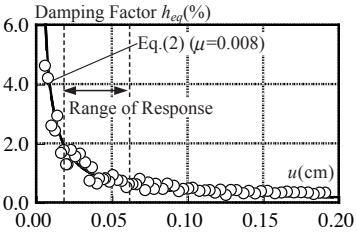

Figure 7: Relationships between damping factors and amplitudes (Es-R_T0.9)

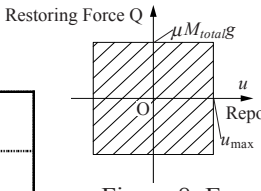

$$h_{eq} = \frac{1}{4\pi}\left(\frac{\Delta W}{W}\right) = \frac{1}{4\pi}\frac{4u_{\max}\mu M_{total}g}{\frac{1}{2}ku_{\max}^2}$$

$$= \frac{2\mu M_{total}g}{\pi k u_{\max}} \propto \frac{1}{u_{\max}} \qquad (1)$$

Figure 8: Energy comsumption by linear motion slider

Table 1: Vibrational characteristics (Es model)

Es Model	T_{eq}(s)	R_T	h_{eq}(%)
R_T0.8	0.053	0.75	1.0
R_T0.9	0.066	0.94	0.9
R_T1.8	0.125	1.77	0.6

Damping Factor h_{eq} is the values subjected to BCJ-L1.

means of the friction damping of linear motion slider which is one of the major factors for the damping. The energy consumption by linear motion slider is shown in Fig.8 and Eq.(1). Therefore, the damping factors at the maximum value of responses subjected to each seismic wave are applied to the damping factor of Es model. Table 1 shows the natural vibrational characteristics for Es model. The damping factors h_{eq} for BCJ-L1 input are about 0.6~1%.

4. Seismic response behavior of cylindrical lattice shells

4.1. Fundamental seismic response behavior of Rs (Shell Roof) model

The maximum response accelerations for Rs0 model on the center line AOA' are shown in Fig.9. The values of CQC method are the accelerations calculated by the response spectrum analysis using CQC method by the modes shown in Fig.5(A1)~(A3). The distribution shapes of vertical acceleration are the antisymmetrical shape, the influences of O1 and O2 modes appear. In the case of horizontal direction, the accelerations are uniformly distributed on AOA'. The values of CQC method approximately agree with the experimental values by MC and accelerometer. Next, the distributions of maximum response accelerations for Rs0 model are shown in Fig.10. The distribution shape of vertical acceleration is almost symmetry to the ridge BOB'. On the other hand, in the case of horizontal direction, the accelerations are approximately uniformly distributed. However, the positions with maximum values appear irregularly.

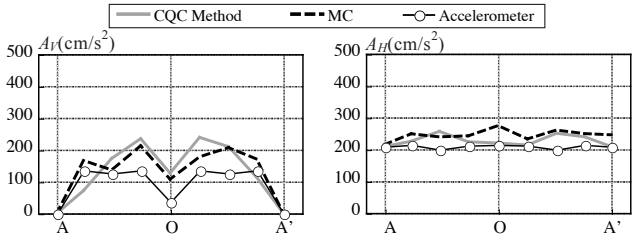

(A) Vertical Acceleration (B) Horizontal Acceleration

Figure 9: Maximum response accelerations for Rs0 model (AOA', ϕ=0deg., BCJ-L1)

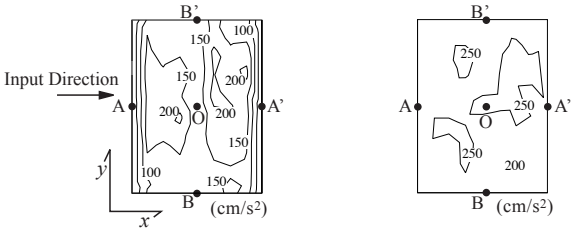

(A) Vertical Acceleration (B) Horizontal Acceleration

Figure 10: Distributions of maximum response accelerations for Rs0 model (ϕ=0deg., BCJ-L1)

4.2 Effects of input direction and natural period ratio on seismic response behavior

Fig.11 shows the maximum response acceleration amplification factors on the center line AO and the ridge BO. The maximum response acceleration amplification factors are obtained from the maximum response accelerations A_V, A_H divided by the maximum response accelerations of Es model A_{eq} ($A_{V,H}/A_{eq}$). The horizontal directions are the input directions of earthquake motions. The horizontal amplification factors are almost constant on the center line and ridge. On the other hand, the vertical amplification factors on the center line AO have a maximum values as the input angle ϕ is 0 deg.. The amplification factor decreases as the input angle increases. In the case of ϕ=90 deg., the factors have a minimum values. In the case of ϕ=0 deg. and 45 deg., the acceleration amplification factors of R_T0.9 model

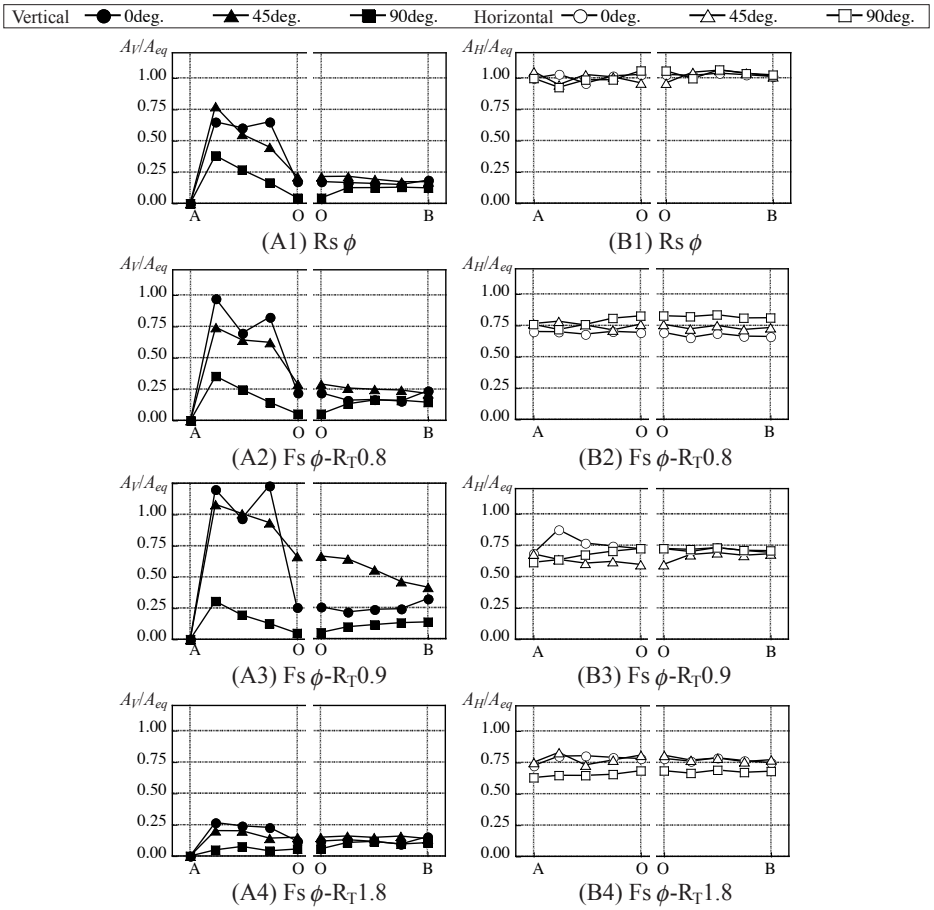

Figure 11: Maximum response acceleration amplification factors on center line AO and ridge BO (BCJ-L1)

amplify due to a resonance of shell roof and substructure. However amplification factors of ϕ=90 deg. are almost constant regardless of the natural period ratio R_T. The vertical amplification factors on ridge BO are about 0.25 except for Fs45-RT0.9 model, these values are small. The amplification factors for Fs45-RT0.9 model have a maximum value at center node O due to the asymmetrical mode as shown in Fig.6.

Fig.12 shows the maximum response displacement amplification factors on the center line AOA'. The maximum response displacement amplification factors are obtained from the maximum response displacements δ_V, δ_H of shell roof including displacements of substructure divided by the maximum response displacements of Es model D_{eq} ($\delta_{V,H}/D_{eq}$). The horizontal directions are the input directions of earthquake motions. The amplification factors for RT0.8 and RT0.9 models are almost equal. However, the factors of RT1.8 model with large natural period ratio are smaller as in the case of response acceleration amplification factors.

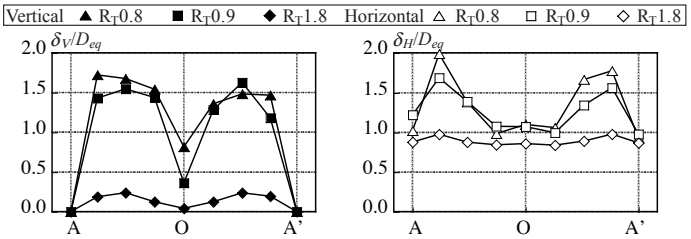

(A) Vertical Amplification Factor (B) Horizontal Amplification Factor

Figure 12: Maximum response displacement amplification factors on center line AOA' for Fs0 model (ϕ=0deg., BCJ-L1)

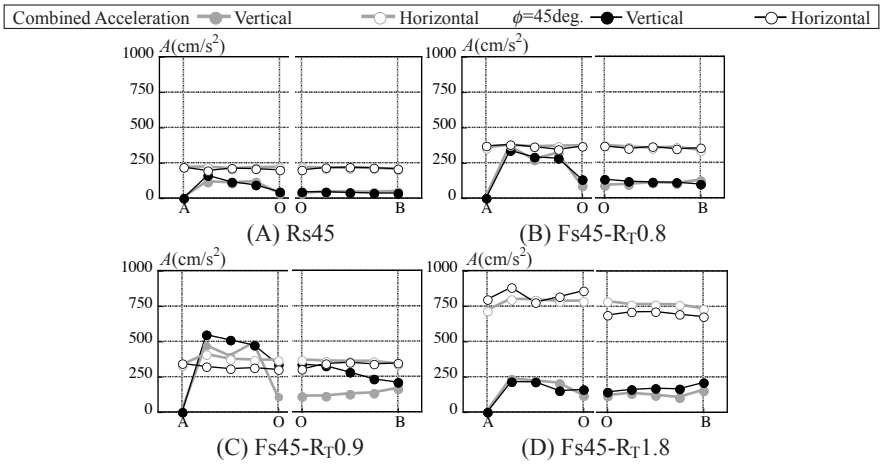

(A) Rs45 (B) Fs45-RT0.8

(C) Fs45-RT0.9 (D) Fs45-RT1.8

Figure 13: Comparisons between combined accelerations derived from maximum response accelerations under input in 0deg. and 90deg. directions and response accelerations under input in 45deg. direction (on center line AO and ridge BO, BCJ-L1)

Next, estimating the response accelerations under seismic motion with input angle ϕ=45 deg. by combining the responses at input angles ϕ=0 deg. and 90 deg. are examined. The response accelerations $A^i_{V\phi}, A^i_{H\phi}$ at node i at input angle ϕ are obtained by Eqs.(2) and (3).

$$A^i_{V\phi} = \left|A^i_{V0}\right|\cos\phi + \left|A^i_{V90}\right|\sin\phi \quad (2) \qquad A^i_{H\phi} = \sqrt{(\left|A^i_{Hx0}\right|\cos\phi)^2 + (\left|A^i_{Hy90}\right|\sin\phi)^2} \quad (3)$$

Fig.13 shows the comparisons between combined accelerations derived from maximum response accelerations under inputs in 0 deg. and 90 deg. directions and response accelerations under input in 45 deg. direction on center line AO and ridge BO. The estimated accelerations by Eqs.(2) and (3) agree with the responses under input in 45 deg. direction except for vertical acceleration on ridge BO for R_T0.9 model.

5. Applicability of previous seismic response evaluation method

In this chapter, it is confirmed that the seismic response evaluation methods proposed in previous papers (Takeuchi *et al*. [1] ~ Takeuchi *et al*. [3]) apply to the responses subjected to earthquake motions with arbitrary direction by shaking table tests. The response amplification factors F_{RV}, F_{RH} are defined as the ratios of maximum response accelerations on shell roof A_{Vmax}, A_{Hmax} to maximum response accelerations of Es models A_{eq}, as shown by Eqs.(4) and (5) (Takeuchi *et al*. [1], Suzuki *et al*. [2]).

$$\text{Vertical: } F_{RV} = A_{Vmax}/A_{eq}\,C_V\theta \quad (4) \qquad \text{Horizontal: } F_{RH} = A_{Hmax}/A_{eq} \quad (5)$$

where C_V is the constant for half subtended angle θ (C_V = 1.33 (input angle ϕ=0 deg.), 0.90(ϕ=90 deg.)). Unit of θ is radian.

Fig.14 shows the relationships between response amplification factors and natural period ratios. In the figures, the evaluation formulae for response amplification ratios proposed in previous papers (Takeuchi *et al*. [1] ~ Takeuchi *et al*. [3]) are also shown. Here, the modes of shell roofs used for evaluating the natural period ratios of Fs0 and Fs90 are the 2nd modes of Rs0 and Rs90 respectively. The experimental values are slightly smaller than the values of evaluation formulae. However, the relationships between the response amplification factors and the natural period ratios of both values show similar tendencies. Compari-

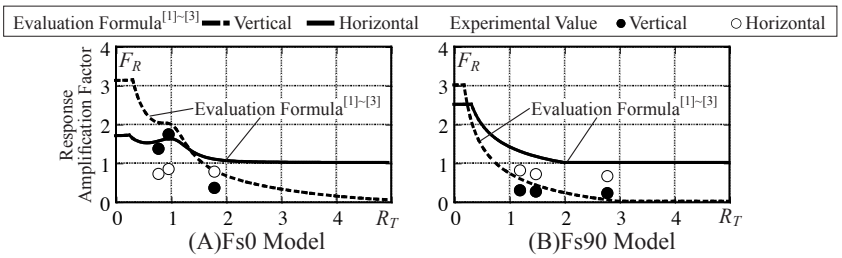

Figure 14: Relationships between response accelerations amplification factors F_R and natural period ratios R_T (BCJ-L1)

sons between the experimental values and the values of evaluation formulae of response amplification factors for each seismic wave are shown in Fig.15. The values of evaluation formulae are in approximate agreement with the experimental results regardless of natural period ratio R_T, input angle ϕ and input seismic motion.

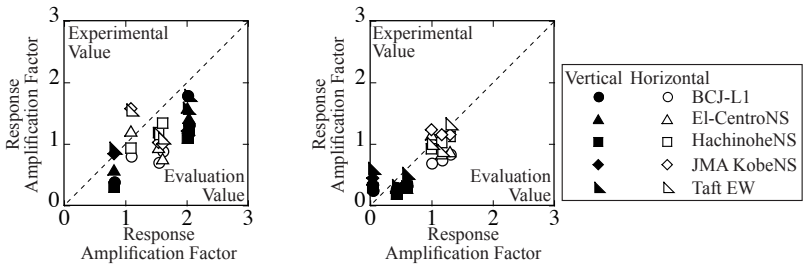

(A)Fs0 Model (B)Fs90 Model

Figure 15: Comparisons between experimental values and evaluation values of maximum response accelerations amplification factors (five seismic waves)

Next, the maximum response accelerations for each node by seismic response evaluation method (Takeuchi *et al*. [1], Suzuki *et al*. [2]) are compared with those by experiments. The prediction formulae for the distributions of response accelerations of shell roof are proposed as Eqs.(6)~(9) by using response amplification factors F_R.

ϕ=0deg. Vertical:
$$A_{RV}(x,y) = A_{eq} F_{RV} C_V \theta \sin\pi\left(\frac{2x}{L_x}\right)\cos\pi\left(\frac{y}{L_y}\right) \tag{6}$$

Horizontal:
$$A_{RH}(x,y) = A_{eq}\left\{1+(F_{RH}-1)\cos\pi\left(\frac{x}{L_x}\right)\cos\pi\left(\frac{y}{L_y}\right)\right\} \tag{7}$$

ϕ=90deg. Vertical:
$$A_{RV}(x,y) = A_{eq} F_{RV} C_V \theta \sin\pi\left(\frac{2y}{L_y}\right)\cos\pi\left(\frac{x}{L_x}\right) \tag{8}$$

Horizontal:
$$A_{RH}(x,y) = A_{eq}\left\{1+(F_{RH}-1)\cos\pi\left(\frac{x}{L_x}\right)\right\} \tag{9}$$

where L_x is span of gable (arch) direction, L_y is span of longitudinal direction and x, y are the coordinates of shell roof shown in Fig.2.

Fig.16 shows comparisons of the response accelerations for all nodes on shell roofs. Fig.17 shows the distributions of vertical accelerations for Fs0,45-R$_T$0.9 models. The seismic response evaluation method for Fs45 model is made by combining the response evaluation methods at input angles ϕ=0 deg. and 90 deg. using Eqs.(2) and (3). Though the response accelerations in vertical direction are evaluated slightly smaller, the values by seismic response evaluation method approximately agree with those by shaking table tests. One of the reasons for the differences of response accelerations in vertical direction is that the response

accelerations increase rapidly in the boundary of shell roof in the distributions of experimental results as shown in Fig.17. However, both values are almost similar in the distribution shape. It is possible for the response accelerations of Fs45 model to be estimated with the prediction accuracy of the responses at input angles ϕ=0 deg. and 90 deg. by the seismic response evaluation method made by combining the response evaluation methods at input angles ϕ=0 deg. and 90deg. as shown in Fig.16(A3) and Fig.17(B).

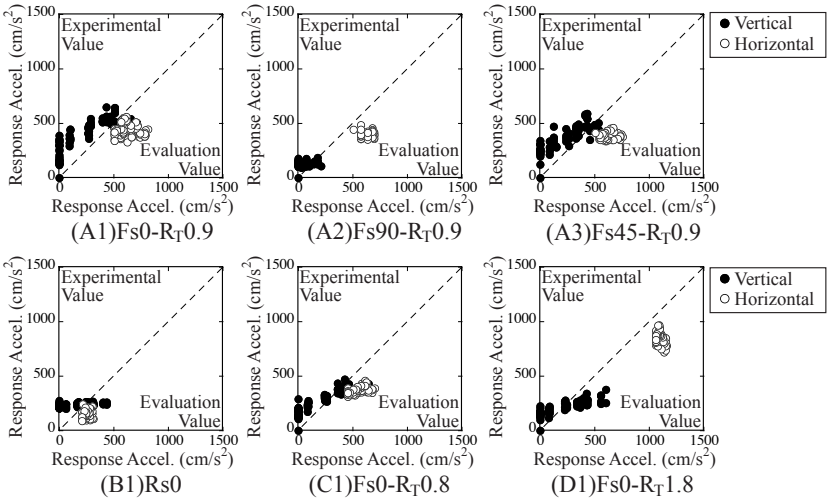

Figure 16: Comparisons between experimental values and evaluation values of response accelerations for all nodes (BCJ-L1)

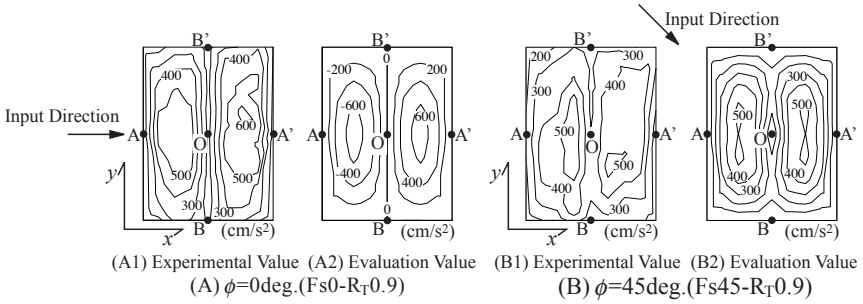

Figure 17: Distributions of maximum vertical response accelerations (BCJ-L1)

6. Conclusions

It is concluded as follows, from the above results.

1) In the case of input in the oblique direction (input angle ϕ=45 deg.), the asymmetrical mode with deformation at the center node O is dominant mode. Unlike inputs in the 0

deg. and 90 deg. directions, the vertical response accelerations occur at the ridge BOB' of shell roof.

2) The vertical response acceleration amplification factors have a maximum values as the input direction of earthquake motion is gable (arch) direction (input angle ϕ=0 deg.). The vertical response acceleration amplification factors of the model that the natural period of shell roof is almost equal to that of equivalent single-mass model amplify due to a resonance. The horizontal response acceleration amplification factors are not significantly influenced by the input direction of earthquake motion.

3) It is possible for the response accelerations and response acceleration amplification factors of cylindrical lattice shell roofs to be estimated by the seismic response evaluation methods proposed in previous papers (Takeuchi *et al*. [1] ~ Takeuchi *et al*. [3]). In the case of input in the oblique direction (input angle ϕ=45 deg.), it is possible for the response accelerations to be estimated with the prediction accuracy of responses under seismic inputs in gable and longitudinal directions (ϕ=0 deg. and 90 deg.) by the seismic response evaluation method made by combining the response evaluation methods at input angles ϕ=0 deg. and 90 deg.

Acknowledgements

The present paper was supported in part by a grant from Grant-in-Aid for Young Scientists (B) (Research No.18760414) and Grant-in-Aid for Scientific Research (B) (Research No.19360247) by Japan Society for the Promotion of Science (JSPS) and research-aid fund by the Japan Iron and Steel Federation (JISF). The experiments in this paper are carried out using the facility by JSPS the 21st Century COE Program "Evolution of Urban Earthquake Engineering".

References

[1] Takeuchi T., Ogawa T., Yamagata C. and Kumagai T., Seismic Response Evaluation of Cylindrical Lattice Roofs with Substructures Using Amplification Factors, *Proceedings of IASS 2005*, Bucharest, 2005, 391-398

[2] Suzuki I., Takeuchi T., Ogawa T. and Kumagai T., Response Evaluation of Cylindrical Lattice Shell Roofs with Substructure Subjected to Earthquake Motions in Longitudinal Direction, *Summaries of Technical Papers of Annual Meeting Architectural Institute of Japan*, B-1, Structures I, 2006, 753-754 (in Japanese)

[3] Takeuchi T., Kumagai T., Shirabe H. and Ogawa T., Seismic Response Evaluation of Lattice Roofs Supported by Multistory Substructures, *Proceedings of IASS 2007*, Venice, 2007, 337-338 (CD-ROM pp.1-9)